JOURNAL OF
Bioactive and Compatible Polymers

Original Article

Journal of Bioactive and Compatible Polymers
2024, Vol. 39(6) 536–550

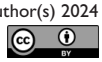

DOI: 10.1177/08839115241267807
journals.sagepub.com/home/jbc


Vitamin E-poly(2-oxazolin)-ciprofloxacin conjugates that enter bacterial cells via their efflux pumps

Alina Romanovska[1], Jonas Tophoven[1], Volker Brandt[1], Marina Breisch[2] and Joerg C. Tiller[1]

Abstract

Rendering established antibiotics by derivatization or formulation is a promising way to quickly obtain higher active antibiotics and to address antibiotic resistant bacterial strains. The antibiotic ciprofloxacin (CIP) conjugated with amphiphilic blockcopoly(2-oxazoline)s (POx) shows greatly enhanced antimicrobial activity, reduces resistance formation, and is active against CIP-resistant bacterial cells with overexpressed efflux pumps. In order to design CIP conjugates with comparable performance, but higher biocompatibility, the hydrophobic POx-block was substituted by a modified α-Tocopherol (VitE), which is predominantly referred to as vitamin E. Modification of VitE with 4-bromomethylbenzoyl bromide leads to a highly active initiator for POx synthesis. Using this initiator for the living cationic polymerization of 2-methyl-2-oxazoline leads to fully end-group functionalized PMOx. Conjugation of these polymers with CIP results in non-cytotoxic conjugates with improved CIP activity. These VitE-PMOx-EDA-xCIP conjugates enter *E. coli* cells via their efflux pumps. In case of *E. coli* with overexpressed efflux pumps (typical for resistant bacteria), the molar activity of the novel CIP conjugates is up to 100 times higher than free CIP, indicating potential of polymer conjugation with antibiotics to overcome bacterial resistances.

[1]Biomaterials and Polymer Science, Department of Bio- and Chemical Engineering, TU Dortmund, Dortmund, Germany
[2]BG University Hospital Bergmannsheil Bochum/Surgical Research, Ruhr University Bochum, Bochum, Germany

Corresponding author:
Joerg C. Tiller, Biomaterials and Polymer Science, Department of Bio- and Chemical Engineering, TU Dortmund, Emil-Figge-Str. 66, Dortmund 44227, Germany.
Email: joerg.tiller@tu-dortmund.de

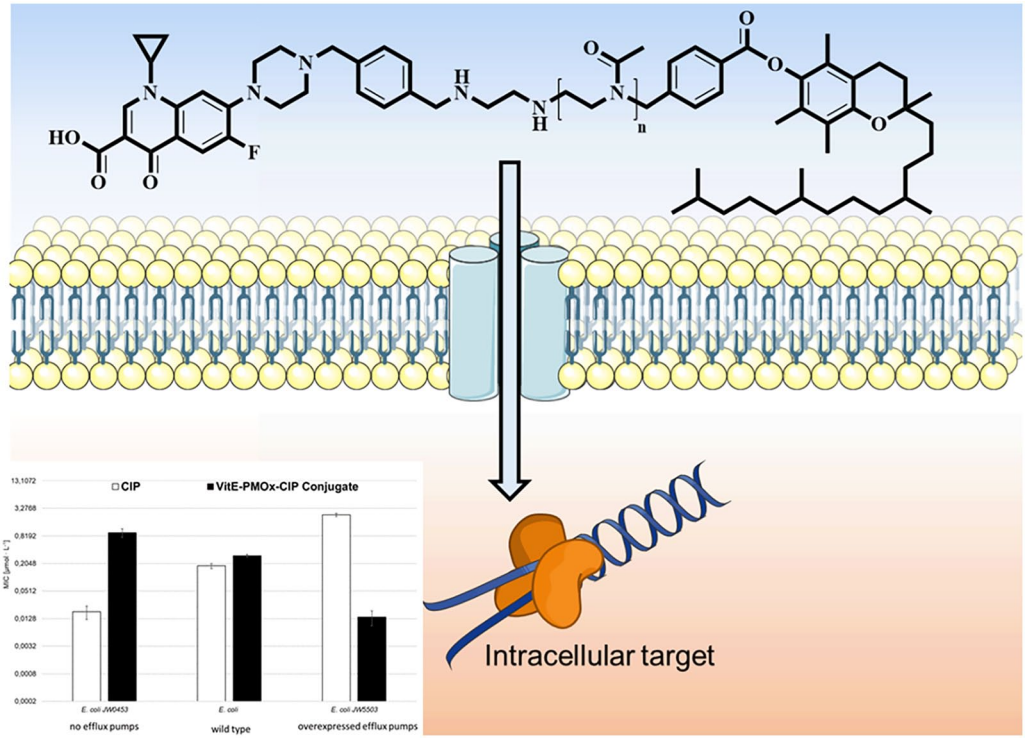

Keywords
α-Tocopherol, poly(2-oxazolines), polymer initiator, living polymerization, ciprofloxacin, bacterial resistances, efflux pumps

Introduction

Bacterial resistance to antibiotics[1] and other biocides[2] is an increasing healthcare problem of the 21st century.[3,4] Since the development of novel antibiotics has almost stopped due to several reasons,[5] the modification and formulation of existing antibiotics is recently in focus of research.[6,7] Among these developments, polymer antibiotic conjugates (PAC) have the potential to alter the properties of antibiotics regarding solubility, toxicity, activity, selectivity, and improvements regarding overcoming existing bacterial resistance and delayed resistance formation.[8–10] Most PACs in the literature are designed to deliver antibiotics toward the infection side or into bacterial cells.[11] To this end, they are commonly attached to the backbone of polymers using functional side groups to form cleavable bonds.[12,13] Often, this construct is not killing bacteria, but the release is realized by an external trigger.[14,15] Alternatively, the antibiotic can be attached onto the end group of a polymer, for example, PEG.[16,17] This allows the antibiotic to be active by reaching its target at the bacterial cell or within a biofilm. The polymer tail can then either protect the antibiotic, help it enter the bacterial cell or can offer the possibility of triggering the activity of the conjugate by changing the shape of the polymer, for example, induced by temperature.[18]

Another polymer that is well suited for end group attachment of drugs is poly (2-oxazoline) (POx).[19–22] We have previously shown that the

conjugation of antibiotics with POx have great potential to improve the performance of the first. While penicillin conjugated to POx becomes resistant against penicillinase degradation,[23] conjugation of ciprofloxacin (CIP) to POx[24] slows the formation of bacterial resistance against these PACs.[25] Varying the structure of POx toward amphiphilic block copolymer structures, greatly activates the conjugated CIP by up to a factor of 20.[26,27] Downside of these amphiphilic CIP-PACs is the strong influence of the conjugated POx on solubility, hemolytic effect on blood cells and cell toxic properties. Depending on the compositions of the block copolymers, the highly active amphiphilic CIP-POx conjugates are either lowly soluble and thus cytotoxic toward stem cells at higher concentrations or well soluble, but somewhat lytic to blood cells. This is critical for a potential formulation of such conjugates. Therefore, we looked for a less toxic hydrophobic function that allows to obtain similarly activated CIP-POx conjugates with improved solubility and cell compatibility.

A promising hydrophobic moiety that is highly biocompatible is the α-Tocopherol, which was discovered by Evans and Bishop in 1922 and is as well as seven other similar compounds referred to as vitamin E.[28] The conjugation of α-Tocopherol (VitE) with polymers not only leads to improved drug delivery properties, but can also contribute to better antimicrobial activity of the polymers.[29] For example, polycationic polymers have shown improved antimicrobial activity against various bacterial strains after conjugation with vitamin E.[29]

In the present work VitE is used as hydrophobic moiety to improve the performance of polymer CIP conjugates with POx.

Results and discussion

The end group modification of POx with bioactive, antimicrobial[30] and/or enzyme inhibiting[31] or binding[32,33] functions has been established in our group by either rendering the initiator[34,35] of the polymerization or the end group.[36] In order to substitute the hydrophobic block in amphiphilic POx-CIP-conjugates with the potentially less toxic α-Tocopherol (VitE), the vitamin was rendered into an initiator for the cationic ring-opening polymerization of 2-oxazolines. To this end, VitE was modified with 4-(bromomethyl)benzoyl bromide (BMB) according to a literature protocol.[29] ^{1}H-NMR analysis and ESI-MS (Supplemental Figures S1 and S2) verify the nature and purity of the targeted compound. The structure of the final conjugates of VitE-PMOx-EDA with xCIP is shown on one example in Figure 1.

First, it was explored whether the novel initiator affords a living polymerization of 2-methyl-2-oxazoline (MOx). To this end, it was reacted with MOx in a molar ratio of 1:30 in deuterated acetonitrile at 110°C. Samples were taken at regular intervals and analyzed by ^{1}H-NMR spectroscopy determining the ratio of MOx in free form and as repeating unit in the formed poly(2-methyl-2-oxazoline) (PMOx). As seen in Figure 2, where $\ln(c_{M,0}/c_M)$ is plotted against reaction time, the reaction follows pseudo-first order kinetics over the whole reaction time until over 99% conversion, which is typical for living polymerizations. The calculated propagation rate constant k_p of the polymerization is calculated to 0.44 M^{-1} min^{-1}.

In order to conjugate the polymer with CIP, the macromolecule was first terminated with ethylene diamine (EDA) after completing polymerization. All signals in the ^{1}H NMR spectrum of this polymer can be assigned to the expected polymer structure, indicating that polymer chains were successfully started with VitE-BMB and functionalized with EDA. The analysis of the obtained ^{1}H-NMR spectrum results in a degree of polymerization of 30 using the signal of the BMB group as reference. This is the exact ratio of molar monomer/initiator suggesting quantitative conversion without chain transfer reaction or undesired termination. The degree of functionalization with EDA was calculated to 97% with respect to the BMB group.

In order to get support the near perfect structure of the targeted polymer with full starting and end group modification, a MALDI-TOF

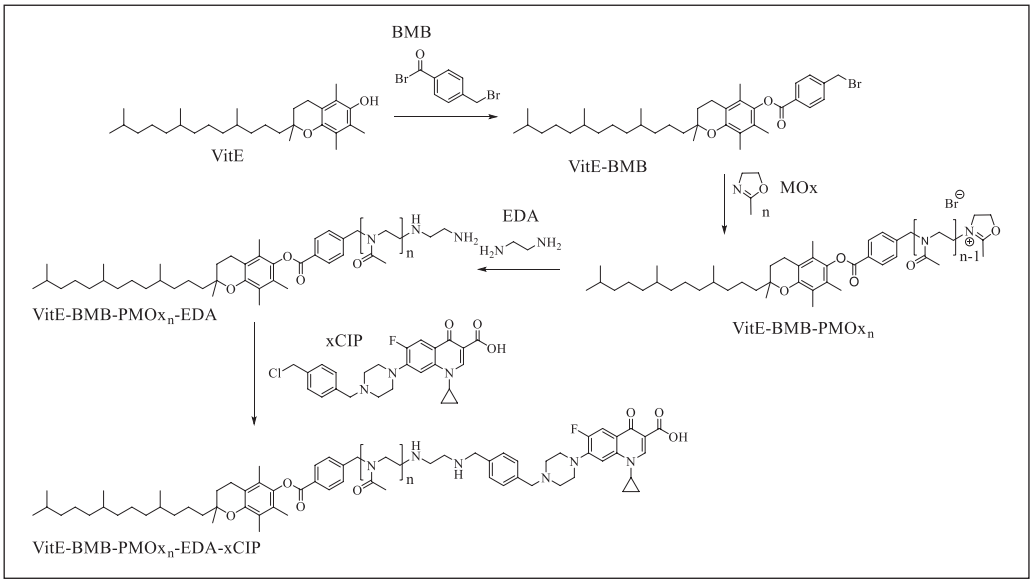

Figure 1. Synthesis route toward VitE-PMOx-EDA-xCIP.

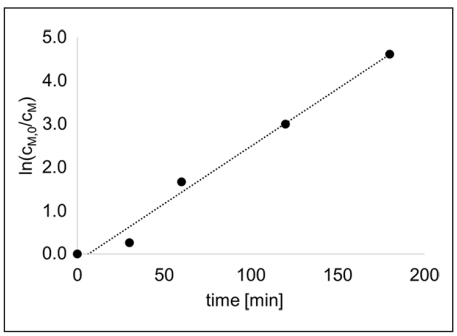

Figure 2. Plot of the determined $\ln(c_{M,0}/c_M)$ values against the reaction time *t* to determine the reaction rate constant of the polymerization of MOx initiated with VitE-BMB in deuterated acetonitrile at 110°C. The conversion rate *p* of MOx was determined by ^{1}H-NMR spectroscopic evaluation by using the integral of MOx units in the polymer and the integral of free MOx to calculate c_{M0}/c_M. Concentration of the initiator was 57 mmol/L.

spectrum was recorded. As shown in Figure 3, only two generations are found in the mass spectrum of the polymer. Both have the mass of MOx as repeating unit (85.4 g/mol) and have a maximum mass of about 3600 g/mol, which is close to the mass calculated from the ^{1}H-NMR spectrum (3200 g/mol). Closer inspection of the individual molecular weights reveals, that one generation can be assigned to the target polymer structure with a potassium counter ion and the other generation represents that of the target structure with a proton counter ion. No chain transfer products or incompletely terminated polymer chains are found in the mass spectrum, indicating that the product is exclusively the target structure.

A series of PMOx with different molecular weight using BMB as initiator and EDA as termination reagent was prepared and subsequently conjugated with CIP. The analytical data collected in Table 1 suggest nearly full conversion with EDA in all cases and conjugation with CIP of more than 90% in most cases.

The prepared CIP conjugates have a varying hydrophilic/hydrophobic balance. It was explored, how this affects the ability to form aggregates. TEM images of dried aqueous solutions of highly concentrated VitE-PMOx-EDA-xCIP conjugates with different PMOx chain lengths depicted in Figure 4 show that conjugates with the highest hydrophobic content form worm-like micelles. Increasing the hydrophilic content results in

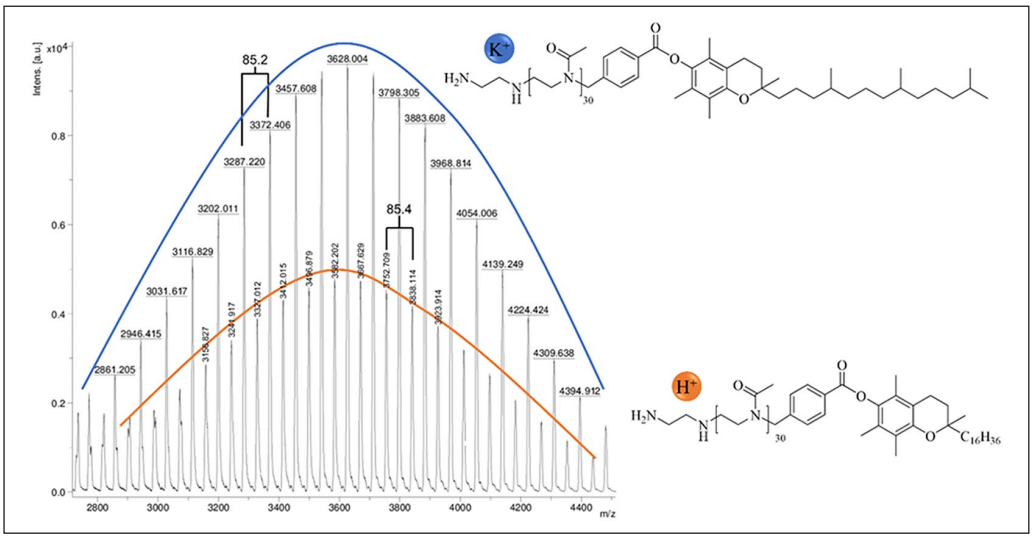

Figure 3. MALDI-TOF of the polymer VitE-PMOx$_{30}$-EDA.

Table 1. Analytical data of VitE-BMB derived CIP PACs characterized by ^{1}H-NMR spectroscopy (the ^{1}H-NMR spectra of the xCIP conjugates are provided in the Supplemental Figures S3 to S6).

PAC	$M_{n,NMR}$ [a] (g/mol)	F_{NMR} [b] (%)
VitE-PMOx$_{10}$-EDA	1500	98
VitE-PMOx$_{22}$-EDA	2300	97
VitE-PMOx$_{30}$-EDA	3200	97
VitE-PMOx$_{56}$-EDA	5200	99
VitE-PMOx$_{90}$-EDA	8300	98
VitE-PMOx$_{11}$-EDA-xCIP	2100	83
VitE-PMOx$_{23}$-EDA-xCIP	3100	90
VitE-PMOx$_{31}$-EDA-xCIP	3800	94
VitE-PMOx$_{56}$-EDA-xCIP	5900	97
VitE-PMOx$_{90}$-EDA-xCIP	8700	90

[a]Degree of polymerization determined by ^{1}H-NMR spectroscopy via comparison of the respective signals caused by the initiating group and the signals caused by the protons of the polymer backbone.
[b]Degree of functionalization determined by ^{1}H-NMR spectroscopy via comparison of the respective signals caused by the initiating and the terminal CIP groups.

spherical micelles of some 10 nm in diameter. Further increasing the length of the PMOx chains leads to the formation of rather undefined larger aggregates (see Figure 4(d)). The critical aggregation concentration CAC of the water-dissolved VitE-PMOx-EDA-xCIP conjugates with higher hydrophobic content was found to be as low as 3.1×10^{-5} mol/L for the PMOx$_{11}$ derivative and 9.5×10^{-5} mol/L for the PMOx$_{31}$ derivative. The CAC values of the conjugates with the larger hydrophilic PMOx chain (PMOx$_{56}$) increase dramatically to 2.2×10^{-2} mol/L. This seems to indicate that the latter conjugates are majorly stabilized in water by unimolecular micelles, which form aggregates composed of more polymer chains only at higher concentrations.

The antibacterial activity of the amphiphilic PACs against several clinically relevant

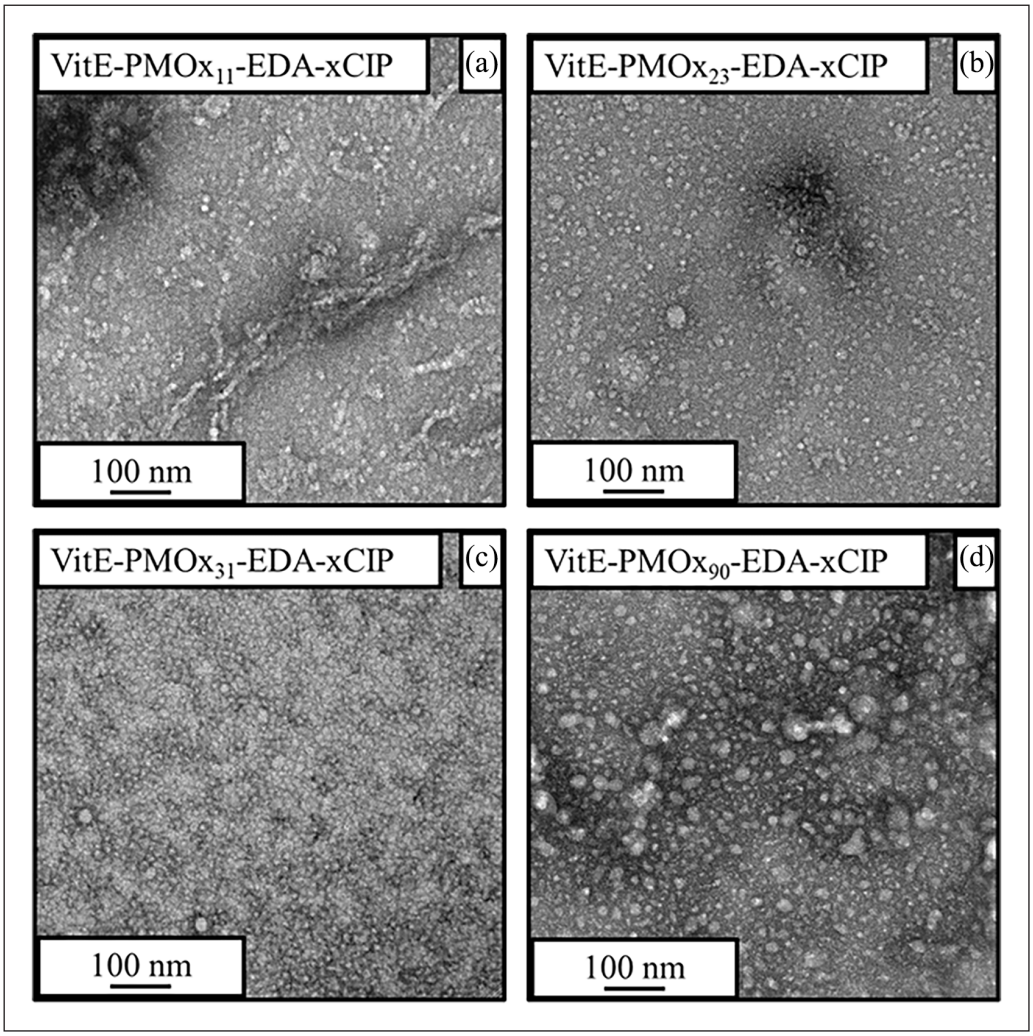

Figure 4. Transmission electron microscopy (TEM) images of the VitE-PMOx-EDA-xCIP conjugates with 11 (a), 23 (b), 31 (c), and 90 (d) repeating units in the polymer. The conjugates were dissolved in water (1 wt%), dropped onto the TEM grids and stained with ruthenium chloride.

infectious and pathogenic bacterial strains (*Staphylococcus aureus* (*S.a.*), *Escherichia coli* (*E.c.*), *Klebsiella pneumoniae* (*K.p.*), *Pseudomonas aeruginosa* (*P.a.*)) was determined using the minimal inhibitory concentration (MIC_{99}) test. The MIC value in our setup corresponds to the concentration at which 99% of the bacteria are inhibited in their growth. This value is compared to the MIC value of CIP. The respective EDA-terminated polymers show no antimicrobial activity against any of the microbial strains (MIC $>500\,\mu g/mL$ in all cases).

The VitE-PMOx-EDA-xCIP conjugates exhibit high antimicrobial activity against all bacterial strains tested (Figure 5). They behave similarly to the previously reported amphiphilic block copolymer POx-xCIP conjugates and much better than the respective hydrophilic PMOx-xCIP-conjugate, showing that the VitE

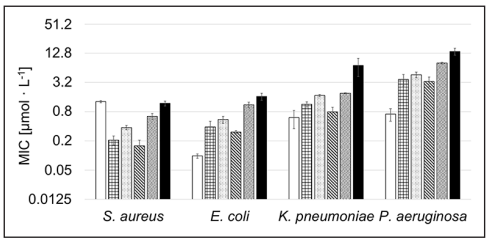

Figure 5. MIC values of CIP (white), checkered: VitE-PMOx$_{11}$-EDA-xCIP, dotted: VitE-PMOx$_{23}$-EDA-xCIP, striped: VitE-PMOx$_{31}$-EDA-xCIP, waved: VitE-PMOx$_{56}$-EDA-xCIP, black: VitE-PMOx$_{90}$-EDA-xCIP.
Values are expressed as mean ± SD ($n = 3$). The numerical MIC values are provided in the Supplemental Tables 1 and 2).

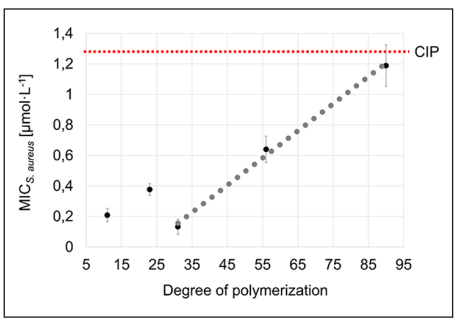

Figure 6. Degree of polymerization (number of repeating units in the polymer chain) against the MIC$_{S.\ aureus}$ value (µg/mL) for VitE-PMOx$_{11}$-EDA-xCIP, VitE-PMOx$_{23}$-EDA-xCIP, VitE-PMOx$_{31}$-EDA-xCIP, VitE-PMOx$_{56}$-EDA-xCIP, VitE-PMOx$_{90}$-EDA-xCIP.
Values are expressed as mean ± SD ($n = 3$).

unit perfectly takes over the role of the hydrophobic POx-Block. Looking at the molecular weight dependence of the conjugates on the antibacterial activity using *S. aureus* as an example reveals that all PACs with a degree of polymerization between 11 and 31 have similar MIC values (Figure 6). A further increase of this chain length to 56 repeating units and higher leads to a strong decrease in antibacterial activity. This correlates with the CAC of the PACs. While conjugates with a shorter PMOx chain form micelles at very low concentrations, the CAC of PMOx chains with a degree of 56 leads

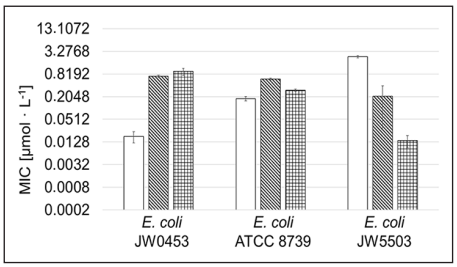

Figure 7. Antimicrobial activity of CIP, PMOx$_{28}$-b-PHptOx$_3$-EDA-xCIP, and VitE-PMOx$_{31}$-EDA-xCIP (checkered) against *E. coli* ATCC 8739 and its mutants, JW0453 without AcrAB-TolC efflux pumps and JW5503 with overexpressed AcrAB-TolC efflux pumps. The MIC-values of CIP (white) and PMOx$_{28}$-b-PHptOx$_3$-EDA-xCIP (striped) are reproduced from a previous study.[26]
All measurements were performed at least in triplicate. Values are expressed as mean ± SD ($n = 3$). PHptOx: poly(2-heptyl-2-oxazoline).

to a more than 100-fold increase in CAC indicating that this PAC does not form multi-chain micelles at concentrations around the MIC. This suggests that the formation of micelles is an important prerequisite for the high antibacterial activity of PACs or at least that strong hydrophobic interactions are required.

One feature of the amphiphilic block copolymer POx-xCIPs is that the polymer chain enables the conjugates to enter the bacterial cells through the AcrAB-TolC efflux pumps of *E. coli* cells and inhibit the CIP target—topoisomerase IV—to kill the bacterial cells. Figure 7 shows the effect of these efflux pumps on CIP and VitE-PMOx$_{31}$-EDA-xCIP in comparison to the amphiphilic PMOx$_{28}$-b-PHptOx$_3$-EDA-xCIP (PHptOx = poly(2-heptyl-2-oxazoline)) against *E. coli* wild-type cells and mutants with deactivated (JW0453) or overexpressed AcrAB-TolC efflux pumps (JW5503).

VitE-PMOx$_{31}$-EDA-xCIP shows good activity against JW0453 but becomes more active as more efflux pumps are expressed. This behavior is exactly the opposite of that observed for CIP, but is consistent with the behavior of the previously reported amphiphilic block copolymer PACs.[26] The conjugate shows 50 times less

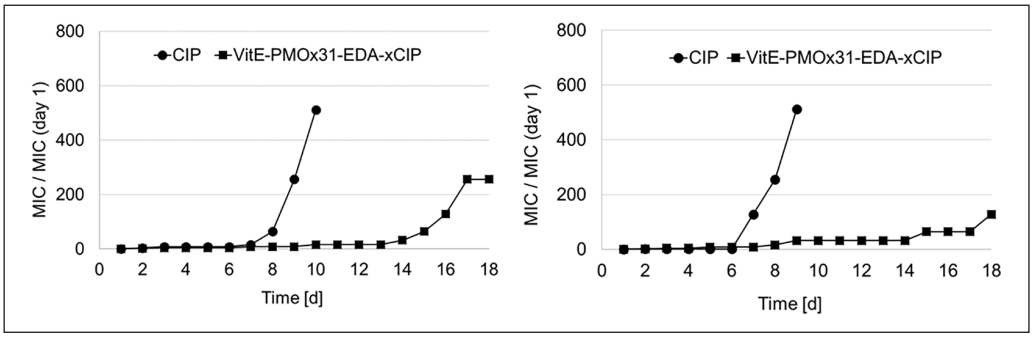

Figure 8. Development of resistance of bacterial cells against free CIP (spheres) and VitE-$PMOx_{31}$-EDA-xCIP (squares) and for (a) *S. aureus* and (b) *E. coli*, respectively. The MIC/MIC (day 1) values are indicating the increased MIC value of the respective bacteria after being treated at MIC/2 in growth medium for 24 h at 37°C.

activity against *E. coli* JW0453 bacteria without efflux pumps than CIP. In contrast, it is 170 times more active than CIP against the bacteria with overexpressed efflux pumps and up to 14 times better active compared to $PMOx_{28}$-b-$PHptOx_3$-EDA-xCIP.[26] Thus, the VitE end group is even improving the ability of the respective CIP PAC to enter *E. coli* cells via their efflux pumps compared to the previously reported amphiphilic CIP PACs.

Since efflux pump overexpression is one of the major resistance mechanisms of bacterial cells to CIP, there is a possibility that VitE-$PMOx_{31}$-EDA-xCIP may have an even lower potential to induce bacterial resistance than the previously reported amphiphilic CIP PACs. The development of bacterial resistance to VitE-$PMOx_{31}$-EDA-xCIP was determined using a modified MIC assay. The test was performed by growing bacterial cells at the highest possible antibiotic concentration (half the MIC) collect them after 24 h and use these cells for the inoculation of the next MIC test. This procedure was repeated for at least 18 days or until MIC levels exceeded 512 times the initial MIC on day 1. *S. aureus* and *E. coli* were selected as representative Gram-positive and Gram-negative test bacteria. The results are shown in comparison to those of CIP (Figure 8).

As seen in Figure 8, after 8–10 days, *S. aureus* and *E. coli* have built up resistance to CIP. After this time almost no resistance was formed by both bacterial strains against the PAC. A notable resistance formed after 14 days of stressing the bacteria with the PAC. Thus, the binding of CIP to PMOx with a VitE end group greatly slows down resistance formation of the typical and clinical relevant bacterial strains *S. aureus* and *E. coli*.

Another important potential of a PAC is that is does not necessarily induce resistance for the respective free antibiotic. As shown previously, simple mutation of the target site does not induce resistance against CIP, but to some extent resistance to the CIP conjugates.[25,26] Thus *S. aureus* cells resistant to the PAC were nearly fully susceptible to the free antibiotic. To investigate, if the here presented VitE-PMOx-EDA-xCIP PAC shows a similar effect, the cross-resistances were explored by determining the MIC value of all formed bacterial strains for CIP and the CIP-PAC VitE-$PMOx_{31}$-EDA-xCIP. As seen in Figure 9, the resistance formation against CIP also leads to a decreased susceptibility toward the CIP-PAC and vice versa. However, in all cases the cross-references induced by one compound are only partially deactivating the other. For example, the resistance of *E. coli* built up against CIP results in an MIC value of some 300 µmol/L.

Having established that the VitE group is capable of strongly activating CIP conjugated

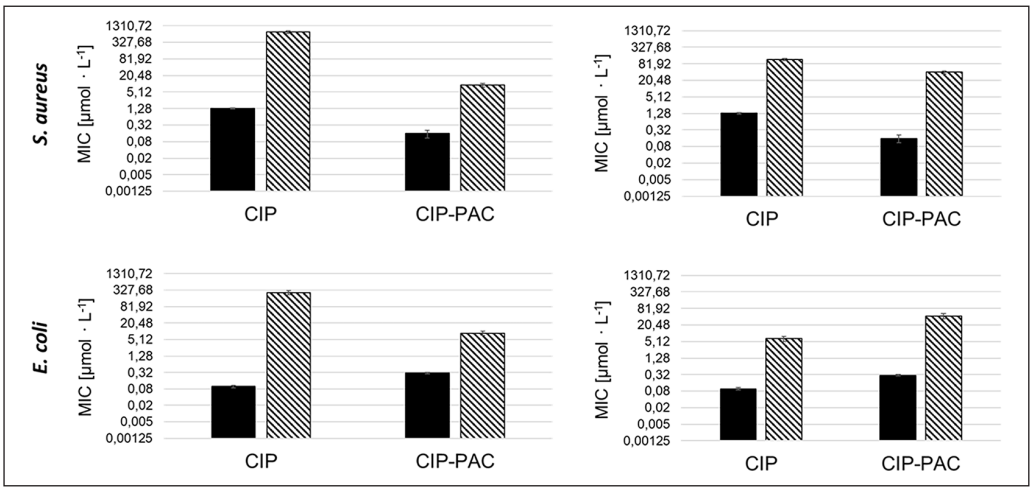

Figure 9. Cross-testing matrix with MIC values of CIP and the conjugate VitE-PMOx$_{31}$-EDA-xCIP for the wild strains (black) and resistant bacterial cells (striped).
Values are expressed as mean ± SD ($n = 3$).

to PMOx, similar to conjugates composed of amphiphilic block copolymer POx-CIP, the effect of this hydrophobic group on the lytic activity toward blood cells was explored. In contrast to the hydrophobic POx chains in the block copolymer PACs, it was expected that the VitE function is not membrane-active due to its branched structure. The blood cell lysis test confirmed this expectation. All VitE-based PACs did not destroy erythrocytes (less than 1-% lysis) even at concentration as high as 20,000 µg/mL. This means that by using VitE instead of hydrophobic poly(2-oxazoline) blocks in POx-CIP conjugates, the cell lytic activity is diminished.

The cytotoxicity of the PACs was tested on rat alveolar macrophages (AM) (NR8383) using the AlamarBlue assay. Macrophages are effector cells of the innate immune system and play an important role in the clearance of pathogens.[37]

In all cases, the cell viability exceeds 80%, indicating that even at such a high concentration as 200 µg/mL the PACs do not induce cytotoxicity in NR8383 after 24 h of incubation (Figure 10).

Conclusions

Goal of this work was to replace the hydrophobic block of highly active amphiphilic block copolymer conjugates of ciprofloxacin (CIP) and poly(2-oxazoline) POx. This was achieved by introducing a novel initiator for the cationic ring-opening polymerization of 2-oxazolines based on α-Tocopherol (VitE). The initiator was used to prepare a series of poly(2-methyl-2-oxazoline) (PMOx)-conjugates with VitE at the start and CIP at the end. These micelle-forming amphiphilic PACs exhibit the high antibacterial activity known from previously reported amphiphilic block copolymer CIP conjugates. In contrast to the latter they are well soluble in water, do not cause cell lysis of erythrocytes even at concentrations as high as 20,000 µg/mL, and are not cytotoxic to macrophages. Additionally, these VitE-PMOx-EDA-xCIP conjugates show a strong tendency to enter Gram-negative *E. coli* cells via their efflux pumps, which leads to greatly increased activity against *E. coli* cells with overexpressed efflux pumps. The VitE-PMOx-EDA-xCIP conjugates are more than 100 times more active

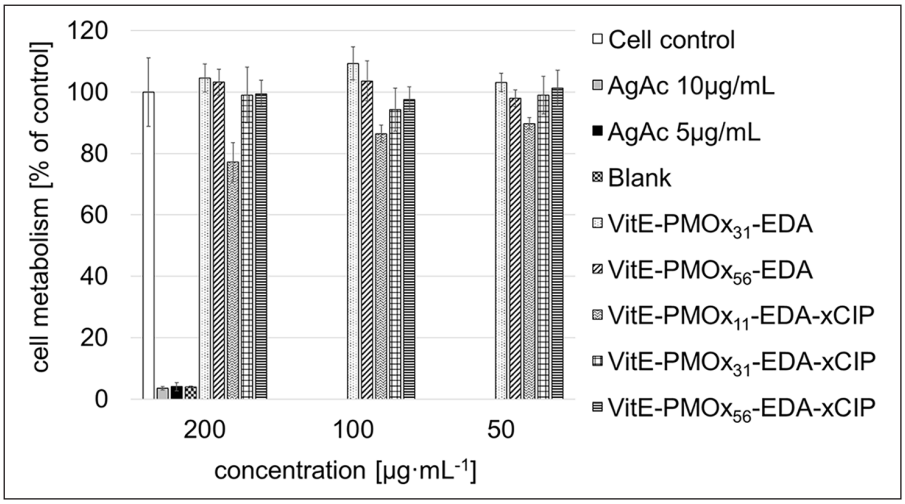

Figure 10. AlamarBlue assay with NR8383 cells treated with white: cells, gray: AgAc 10 µg/mL, black: AgAc 5 µg/mL, black checkered: blank, dotted: VitE-$PMOx_{31}$-EDA, striped: VitE-$PMOx_{56}$-EDA, waved: VitE-$PMOx_{11}$-EDA-xCIP, checkered: VitE-$PMOx_{31}$-EDA-xCIP, cross-strip: VitE-$PMOx_{56}$-EDA-xCIP in RMPI/FCS for 24 h.
Values are expressed as mean ± SD ($n = 3$–4).

against such cells compared to the antibiotic CIP, while the latter is more than 100 times more active than the respective conjugate in case of *E. coli* cells with suppressed efflux pumps. This in combination to the fact that the formation of bacterial resistance against the CIP conjugates is greatly delayed makes the novel conjugates an interesting candidate for a next generation antibiotic.

Materials and methods

Materials

The reactions, purifications and polymerizations were carried out under an inert atmosphere. The distillation of acetonitrile (Fisher Scientific) was carried out from diphosphorus pentoxide (VWR), then from potassium carbonate (VWR), and stored over 3 Å molecular sieves. The water content was determined by Karl Fischer titration (<0.5 ppm). 2-Methyl-2-oxazoline (MOx, ACROS) and Trimethylamine (ACROS) was distilled under reduced pressure from calcium hydride (ACROS). Ethylene diamine (EDA; Alfa Aesar) was distilled under reduced pressure. Dichloromethane (DCM; Fisher Scientific) was dried overnight over calcium chloride and subsequently stored over 3 Å molecular sieves. Methanol (Fisher Scientific), diethyl ether (Fisher Scientific), ethyl acetate (Fisher Scientific), α-Tocopherol (TCI), 4-(bromomethyl)benzoyl bromide (BMB, TCI) were used without further purification. α,α′-Dichloro-p-xylene (TCI) was recrystallized in chloroform. Ciprofloxacin (ACROS), dithranol (Sigma-Aldrich), acetic acid (Merck), sodium hydrogen carbonate (Merck), sodium chloride (Fisher Scientific), sodium dihydrogen phosphate dihydrate (Merck), sodium citrate (Sigma-Aldrich), citric acid mono-hydrate (Sigma-Aldrich), glucose monohydrate (Sigma-Aldrich), sodium hydroxide (VWR), hydrochloric acid (VWR), glycerol (ACROS), triton X-100 (ACROS) and nutrient broth (Roth) were used without further purification. The bacterial strains *Escherichia coli* (Gram-negative, ATCC 25922), *Klebsiella pneumoniae* (Gram-negative, ATCC 13883), *Pseudomonas aeruginosa* (Gram-negative, ATCC 17423), and *Staphylococcus aureus* (Gram-positive, ATCC 25323) were provided by the German Resource Center for Biological Material (DSMZ). *E. coli* ATCC 8739,

E. coli JW0453 and *E. coli* JW5503 were obtained from the Keio collection.

Measurements

^{1}H-NMR spectra were recorded in deuterated solvents ($CDCl_3$) using FT-appliances of Varian type Inova 500 (500 MHz) or FT-appliances of Bruker, types DPX-300 (300 MHz), DRX-400 (400 MHz), DRX-500 (500 MHz). The residual protons of the not fully deuterated solvents served as an internal standard.

The ESI-MS measurements were performed on a LTQ Orbitrap XL (Thermo) mass spectrometer. The polymer samples were dissolved in ethanol at a concentration of 100 µmol/mL. Nominal nitrogen back pressure and ESI voltage were adapted to the respective analyte, varying between 0.4 and 1.4 psi and 1.8 kV, respectively. The profile mass spectra were obtained as full scan data in positive mode by accumulation of 2 µ scans in the mass range *m*/*z* 50–2000 with a resolution of 100,000. The measurement accuracy was <5 ppm (<1 ppm internal log).

The matrix-assisted laser-desorption-ionization time-of-flight (MALDI-TOF) was measured on an Autoflex of the Firma Bruker. The laser was a nitrogen laser with a wavelength of 337.1 nm. The measure control was managed by the FlexControl software. The analysis of the measured spectra was carried out by the software FlexAnalysis. For the sample preparation the dried droplet method was used. The samples (10 mg/mL) and the universal matrix dithranol (10 mg/mL) were dissolved in chloroform. Subsequently, 50 µL were taken from each of the two solutions and mixed separately. After adding acetic acid, a total of 1 µL of the sample solution-universal matrix mix was dropped onto the sample disk. After evaporation of the solvent, 1 µL of the sample solution-universal matrix mix was again dropped onto the sample disk. This procedure was repeated several times. After evaporation of the chloroform, the sample was measured.

The calculation of the theoretical molecular masses was performed by using the following isotopes: ^{12}C = 12.000 g/mol, ^{16}O = 15.995 g/mol^{-1}, ^{14}N = 14.003 g/mol, ^{1}H = 1.008 g/mol, ^{79}Br = 78.918 g/mol, $^{1}H^{+}$ = 1.0072766 g/mol, and K = 38.9637 g/mol.

Transmission electron micrographs were acquired on an Talos F200X microscope operating at an accelerating voltage of 200 kV. The polymer samples were dissolved with 1 wt% in distilled water and dropped on carbon-coated copper grids allowing the solvent to evaporate. A staining solution was prepared as follows. 0.2 g of ruthenium chloride hydrate and 10 mL (5 wt%) sodium hypochlorite were dissolved in 100 mL distilled deionized water. The grids with the polymeric sample were incubated with three droplets of staining solution. After 20 min, the samples were analyzed by transmission electron microscopy (TEM).

Fluorescence spectroscopy for CAC determination. A methanol solution of the fluorescent dye pyrene (0.1 mM) was used for CAC determination. In aqueous solution, a dilution series of the PAC of interest was prepared, halving the concentration with each step. Then, 10 µL of the pyrene-MeOH solution was added. The dilution series was examined by fluorescence spectroscopy (f-2700 from Hitachi at 25°C, excitation wavelength of 310 nm) and the emission intensities at $I_1 = 373$ nm and $I_3 = 383$ nm were measured.[38] The onset of the change of the ratio of I_1/I_3 was considered the CAC value.[39]

Initiator synthesis

In a 250 mL round bottom flask, 5.4 g (19.3 mmol, 1 equiv) of 4-(bromomethyl)benzoyl bromide was dissolved in 50 mL of dry DCM. In a new glass tube, 8.7 mL vitamin E (8.3 g, 19.3 mmol, 1 equiv) and 3 mL triethylamine (21.6 mmol, 1.12 equiv) were dissolved in 50 mL dry DCM.[29] The 50 mL VitE–TEA–DCM solution was then added to the 4-(bromomethyl)benzoyl bromide—DCM solution over 30 min and stirred at room temperature for 18 h. The product was purified by column chromatography with the running medium heptane:ethyl acetate (96%:4%).

^{1}H NMR (500 MHz, Chlorofom-d) δ ppm = 0.84–0.95 (m, 12 H) 1.07–1.21 (m, 5 H) 1.22–1.37 (m, 14 H) 1.38–1.47 (m, 3 H) 1.53–1.67 (m, 2 H) 1.76–1.91 (m, 2 H) 2.00–2.12 (m, 6 H) 2.12–2.21 (m, 3 H) 2.60–2.69 (m, 2 H) 4.56 (s, 2 H) 7.54–7.61 (m, 2 H) 8.23–8.30 (m, 2 H).

General procedure for the polymerization

The starting concentration of the monomer was varied to set the desired degree of polymerization DP_{set} according to [initiator] = [monomer]·DP_{set} − 1. For example, the initiator VitE-4-(bromomethyl) benzoyl bromide (0.63 g, 1 mmol, 1 equiv) was dissolved in acetonitrile (15 mL) at room temperature, and the monomer 2-methyl-2-oxazoline was added (2.55 g, 30 mmol, 30 equiv) to the solution. The polymerization was carried out in a CEM Discover synthetic microwave. The reaction temperature was monitored with a vertically focused IR temperature sensor. The vessels were heated to 110°C for 4 h in order to use the power (150 W) with magnetic stirring. Performance was reduced to a base level after the desired temperature was reached while maintaining the target temperature. The vessels were cooled by compressed air shocks during the polymerization to maintain the set temperature. To terminate the living polymer chains, a 10-fold molar excess (based on the initiator molarity) of ethylene diamine was added and heated at 45°C for 72 h. The polymer was then precipitated in diethyl ether and dialyzed in MeOH using benzoylated cellulose membranes (1000 MWCO). The water was removed by reduced pressure, and the products were obtained as white solids in yields of 69%–93%.

VitE-PMOx$_{30}$-EDA ^{1}H NMR (400 MHz, chloroform-*d*) δ ppm = 0.73–0.87 (m, 12 H) 0.97–1.14 (m, 5 H) 1.14–1.29 (m, 14 H) 1.29–1.42 (m, 3 H) 1.49 (dt, *J* = 13.35, 6.60 Hz, 2 H) 1.79 (s, 2 H) 1.88–1.98 (m, 6 H) 1.99–2.19 (m, 80 H) 2.58 (t, *J* = 6.56 Hz, 2 H) 2.62–2.85 (m, 6 H) 3.23–3.84 (m, 105 H) 4.76 (s, 2 H) 7.49 (d, *J* = 8.54 Hz, 2 H) 8.18 (d, *J* = 8.24 Hz, 2 H).

7-(4-(4-(Chloromethyl)benzyl) piperazin-1-yl)-1-cyclopropyl-6-fluoro-4-oxo-1,4 dihydroquino-line-3-carboxylic acid (xCIP-Spacer)

The xCIP spacer was synthesized according to literature by reacting CIP with α,α′-dichloro-*p*-xylol.[24] Briefly, α,α′-Dichloro-*p*-xylene (875 mg, 5.00 mmol, 5 equiv) and $NaHCO_3$ (168 mg, 2 mmol, 2 equiv) were dissolved in a mixture of *N,N*-dimethylformamide and MeCN (1:1, 4 mL). Ciprofloxacin (331 mg, 1.00 mmol, 1 equiv) was added to the solution at room temperature. The reaction mixture was stirred at 80°C for 24 h and the product was precipitated in Et_2O and purified by column chromatography (SiO_2; CH_2Cl_2:MeOH = 20:1).

General procedure of xCIP-linking

The synthesis of the xCIP-Linking with polymers was carried out according to the literature.[24] Briefly, xCIP (93.8 mg, 0.2 mmol, 2 equiv) and $NaHCO_3$ (16.8 mg, 0.2 mmol, 2 equiv) were suspended in a mixture of *N,N*-dimethylformamide and acetonitrile (1:1, 4 mL). One equivalent of the respective EDA terminated polymer was added to the suspension at room temperature. The reaction mixture was stirred at 80°C for 24 h. The product was precipitated in Et_2O, dried, re-dissolved in water and dialyzed against water in membranes of Roth (ZelluTrans) with a molecular cut-off of 2000 g/mol.

Minimal inhibitory concentration, resistance-test, cross-test and hemocompatibility-test

The investigation of the antimicrobial activity, resistance, and the cross-test hemocompatibility of the polymer-antibiotic-conjugates was carried out according to the literature.[24] The hemocompatibility-test (HC_{50}) was slightly adopted. Thereby, the absorbance at 541 nm (<0.12) of the nearly colorless solution

obtained after 1 h of incubation at 37°C of the blood cells in the buffer followed by centrifugation was taken as negative control and was subtracted from all measured absorbance values. The positive control was obtained by treating the blood cells with 2 µL Triton X for 1 h. The absorbance of the supernatant was 26.68 ± 5.88 (calculated from the determined absorbance of a diluted sample). This value was considered as 100% lysis.

Cell culture

Cell experiments were performed with the cell line NR8383 (rat alveolar macrophages; LGC Standards GmbH, Wesel, Germany). Cells cultivation was carried out in Ham's F-12 medium with 15% fetal calf serum (FCS; GIBCO; Invitrogen, Karlsruhe, Germany) in 175 cm^2 cell culture flasks (BD Falcon; Becton Dickinson GmbH, Heidelberg, Germany) at standard cell culture conditions (humidified atmosphere, 37°C, 5% CO_2). The NR8383 cells were partly adherent and partly non-adherent, with a ratio between adherent and non-adherent cells about 1:1. For cell experiments, adherent cells were detached from the cell culture flasks with a TPP cell scraper (TPP Techno Plastic Products AG, Trasadingen, Switzerland), combined with non-adherent cells and seeded into 24-well cell culture plates (BD Falcon) at a cell concentration of 5×10^5 cells/mL.

AlamarBlue assay

After exposure to polymer antibiotic conjugates for 24 h, the cell metabolic activity of NR8383 was analyzed by the AlamarBlue assay. Therefore, cells were incubated with the AlamarBlue reagent (1 + 10 in Ham's F-12/15% FCS) for 2 h under cell culture conditions. Subsequently, fluorescence intensity was analyzed at 590 nm using a microplate reader (FLUOstar Optima; BMG LABTECH GmbH, Ortenberg, Germany). The fluorescence intensity of the cell culture incubated without additives was found to be 25,400 ± 3491 (negative control). After treating NR8383 cells with 5 µg/mL silver acetate (24 h, toxic conditions), the fluorescence intensity drops below 1000 (positive control). The data are expressed as the mean ± standard deviation (SD) of at least three independent experiments and given as percentage of the untreated cells cultured in Ham's F-12/15% FCS without additives.

Authors' note

This work is dedicated to Raphael Martin Ottenbrite.

Acknowledgements

All polymers were synthesized using CEM Discover microwaves, which were kindly provided by CEM for ungraduated student education. The authors thank Dr. Wolf Hiller and his team from the department of chemistry for recording the NMR spectra and Dr. Sebastian Zühlke and his team from the Center for Mass Spectrometry (CMS) for recording the ESI-MS spectra at the TU Dortmund. The authors also thank the butcher shop Schultenhof, Dortmund, for providing fresh porcine blood.

Author contributions

J.C.T. and A.R. designed the study, interpreted the results and wrote the manuscript. A.R. carried out the synthesis of the VitE-PMOx-EDA-xCIP and the resistance tests. A.R. and J.T. carried out the MIC tests with the PACs. M.B. and A.R. performed the AlamarBlue assay. V.B. has performed all TEM recordings.

Declaration of conflicting interests

The author(s) declared no potential conflicts of interest with respect to the research, authorship, and/or publication of this article

Funding

The author(s) disclosed receipt of the following financial support for the research, authorship, and/or publication of this article: The TEM was in part financed by the DFG in grant INST 212/423-1 FUGG.

ORCID iD

Joerg C. Tiller https://orcid.org/0000-0002-1531-0795

Supplemental material

Supplemental material for this article is available online.

References

1. Morrison L and Zembower TR. Antimicrobial resistance. *Gastrointest Endosc Clin N Am* 2020; 30(4): 619–635.
2. Maillard J-Y and Pascoe M. Disinfectants and antiseptics: mechanisms of action and resistance. *Nat Rev Microbiol* 2024; 22(1): 4–17.
3. de Kraker M, Stewardson A and Harbarth S. Will 10 million people die a year due to antimicrobial resistance by 2050?. *PLoS Med* 2016; 13(11): e1002184.
4. Uddin TM, Chakraborty AJ, Khusro A, et al. Antibiotic resistance in microbes: history, mechanisms, therapeutic strategies and future prospects. *J Infec Public Health* 2021; 14(12): 1750–1766.
5. Hegemann JD, Birkelbach J, Walesch S, et al. Current developments in antibiotic discovery. *EMBO Rep* 2023; 24(1): e56184.
6. Elfadil D, Elkhatib WF and El-Sayyad GS. Promising advances in nanobiotic-based formulations for drug specific targeting against multidrug-resistant microbes and biofilm-associated infections. *Microb Pathog* 2022; 170: 105721.
7. Majhi S and Das D. Chemical derivatization of natural products: semisynthesis and pharmacological aspects—a decade update. *Tetrahedron* 2021; 78: 131801.
8. Varvarà P, Calà C, Maida CM, et al. Arginine-rich peptidomimetic ampicillin/gentamicin conjugate to tackle nosocomial biofilms: a promising strategy to repurpose first-line antibiotics. *ACS Infect Dis* 2023; 9(4): 916–927.
9. Thottathil S, Puttaiahgowda YM and Kanth S. Advancement and future perspectives on ampicillin-loaded antimicrobial polymers—a review. *J Drug Deliv Sci Technol* 2023; 81: 104227.
10. Kanth S, Malgar Puttaiahgowda Y and Gupta S. Recent advancements and perspective of ciprofloxacin-based antimicrobial polymers. *J Biomater Sci Polym Ed* 2023; 34(7): 918–949.
11. Tharmatt A, Chhina A, Saini M, et al. Novel therapeutics involving antibiotic polymer conjugates for treating various ailments: a review. *ASSAY Drug Dev Technol* 2022; 20(4): 137–148.
12. Zhang R, Jones MM, Moussa H, et al. Polymer–antibiotic conjugates as antibacterial additives in dental resins. *Biomater Sci* 2019; 7(1): 287–295.
13. Turos E, Shim J-Y, Wang Y, et al. Antibiotic-conjugated polyacrylate nanoparticles: new opportunities for development of anti-MRSA agents. *Bioorg Med Chem Lett* 2007; 17(1): 53–56.
14. Ye M, Zhao Y, Wang Y, et al. pH-responsive polymer–drug conjugate: an effective strategy to combat the antimicrobial resistance. *Adv Funct Mater* 2020; 30(39): 2002655.
15. Zhou Q, Si Z, Wang K, et al. Enzyme-triggered smart antimicrobial drug release systems against bacterial infections. *J Control Release* 2022; 352: 507–526.
16. Du J, Bandara HMHN, Du P, et al. Improved biofilm antimicrobial activity of polyethylene glycol conjugated tobramycin compared to tobramycin in Pseudomonas aeruginosa biofilms. *Mol Pharm* 2015; 12(5): 1544–1553.
17. Lawson MC, Shoemaker R, Hoth KB, et al. Polymerizable vancomycin derivatives for bactericidal biomaterial surface modification: structure−function evaluation. *Biomacromolecules* 2009; 10(8): 2221–2234.
18. Chang J, Chen Y, Xu Z, et al. Switchable control of antibiotic activity: a shape-shifting "tail" strategy. *Bioconj Chem* 2018; 29(1): 74–82.
19. Morrow JP, Mazrad ZAI, Bush AI, et al. Poly(2-oxazoline)—ferrostatin-1 drug conjugates inhibit ferroptotic cell death. *J Control Release* 2022; 350: 193–203.
20. Sedlacek O, Van Driessche A, Uvyn A, et al. Poly(2-methyl-2-oxazoline) conjugates with doxorubicin: from synthesis of high drug loading water-soluble constructs to in vitro anticancer properties. *J Control Release* 2020; 326: 53–62.
21. Tang J, Cheng Y, Huang T, et al. Simultaneous deposition of tannic acid derivative and covalent conjugation of poly(2-methyl-2-oxazoline) for the construction of antifouling coatings. *Colloids Surf B Biointerfaces* 2023; 224: 113194.
22. Zhou M, Cui R, Luo Z, et al. Convenient and controllable synthesis of poly(2-oxazoline)-conjugated doxorubicin for regulating antitumor selectivity. *J Funct Biomater* 2023; 14(7): 382.
23. Schmidt M, Bast LK, Lanfer F, et al. Poly(2-oxazoline)-antibiotic conjugates with penicillins. *Bioconjug Chem* 2017; 28(9): 2440–2451.

24. Schmidt M, Harmuth S, Barth ER, et al. Conjugation of ciprofloxacin with poly (2-oxazoline) s and polyethylene glycol via end groups. *Bioconjug Chem* 2015; 26(9): 1950–1962.
25. Schmidt M, Romanovska A, Wolf Y, et al. Insights into the kinetics of the resistance formation of bacteria against ciprofloxacin poly(2-methyl-2-oxazoline) conjugates. *Bioconjug Chem* 2018; 29(8): 2671–2678.
26. Romanovska A, Keil J, Tophoven J, et al. Conjugates of ciprofloxacin and amphiphilic block copoly (2-alkyl-2-oxazolines) s overcome efflux pumps and are active against CIP-resistant bacteria. *Mol Pharm* 2021; 18(9): 3532–3543.
27. Romanovska A, Schmidt M, Brandt V, et al. Controlling the function of bioactive worm micelles by enzyme-cleavable non-covalent inter-assembly cross-linking. *J Control Release* 2024; 368: 15–23.
28. Evans HM and Bishop KS. On the existence of a hitherto unrecognized dietary factor essential for reproduction. *Science* 1922; 56(1458): 650–651.
29. Ng VWL, Ke X, Lee ALZ, et al. Synergistic co-delivery of membrane-disrupting polymers with commercial antibiotics against highly opportunistic bacteria. *Adv Mater* 2013; 25(46): 6730–6736.
30. Richter L, Hijazi M, Arfeen F, et al. Telechelic, antimicrobial hydrophilic polycations with two modes of action. *Macromol Biosci* 2018; 18(4): 1700389.
31. Hijazi M, Krumm C, Cinar S, et al. Entropically driven polymeric enzyme inhibitors by end-group directed conjugation. *Chem Eur J* 2018; 24(18): 4523–4527.
32. Hijazi M, Spiekermann P, Krumm C, et al. Poly(2-oxazoline)s terminated with 2,2′-imino diacetic acid form noncovalent polymer–enzyme conjugates that are highly active in organic solvents. *Biotechnol Bioeng* 2019; 116(2): 272–282.
33. Konieczny S, Fik CP, Averesch NJH, et al. Organosoluble enzyme conjugates with poly(2-oxazoline)s via pyromellitic acid dianhydride. *J Biotechnol* 2012; 159(3): 195–203.
34. Fik CP, Konieczny S, Pashley DH, et al. Telechelic poly(2-oxazoline)s with a biocidal and a polymerizable terminal as collagenase inhibiting additive for long-term active antimicrobial dental materials. *Macromol Biosci* 2014; 14(11): 1569–1579.
35. Fik CP, Krumm C, Muennig C, et al. Impact of functional satellite groups on the antimicrobial activity and hemocompatibility of telechelic poly(2-methyloxazoline)s. *Biomacromolecules* 2012; 13(1): 165–172.
36. Bieser AM, Thomann Y and Tiller JC. Contact-active antimicrobial and potentially self-polishing coatings based on cellulose. *Macromol Biosci* 2011; 11(1): 111–121.
37. Scherbart A, Schins R, van Berlo D, et al. Partikel–Makrophagen–Interaktionen: Untersuchungen zu oxidativem Stress und Entzündung. *Pneumologie* 2009; 63(Suppl 01): P291.
38. Kalyanasundaram K and Thomas J. Environmental effects on vibronic band intensities in pyrene monomer fluorescence and their application in studies of micellar systems. *J Am Chem Soc* 1977; 99(7): 2039–2044.
39. Maiti S, Chatterji PR, Nisha CK, et al. Aggregation and polymerization of PEG-based macromonomers with methacryloyl group as the only hydrophobic segment. *J Colloid Interf Sci* 2001; 240(2): 630–635.